UDK
Original scientific article/Izvirni znanstveni članek

ISSN 1580-2949
MTAEC9, 58(3)433(2024)

# FATIGUE BEHAVIOUR OF COPPER-BRAZED 316L STAINLESS STEEL

## UTRUJANJE BAKRENEGA LOTNEGA SPOJA Z NERJAVNIM JEKLOM 316L

**Jernej Kralj[1], Blaž Hanželič[1], Srečko Glodež[1*], Janez Kramberger[1], Roman Satošek[2], Branko Nečemer[1]**

[1]University of Maribor, Faculty of Mechanical Engineering, Smetanova 17, 2000 Maribor, Slovenia
[2]Danfoss Trata d.o.o, Korenova 5, SI-1241 Kamnik, Slovenia

*Prejem rokopisa – received: 2023-11-02; sprejem za objavo – accepted for publication: 2024-04-24*

doi:10.17222/mit.2023.1036

The plate heat exchanger (PHE) is a component that provides heat to be transferred from hot water to domestic cold water without mixing them with high efficiency. Over the lifetime of the PHE, cyclic pressure acts on the brazing points and the plates, and this can lead to fatigue failure. The fatigue behaviour of the PHE, designed by using copper-brazed 316L (also known as 1.4404) stainless steel, was investigated by performing fatigue tests to obtain the S-N curve of the analysed brazed joint. The fatigue tests were performed on a Vibrophore 100 testing machine under the load ratio $R = 0.1$ for different values of calculated amplitude stress. Based on the obtained experimental results, an appropriate material model of the analysed brazed joint was created, which was validated with a numerical calculation in the framework of a program code Ansys. A validated material model can then be used for the subsequent numerical analysis of the PHE.

Keywords: plate heat exchanger, brazed joint, fatigue, experimental testing

Ploščni toplotni izmenjevalec je naprava, ki se uporablja za prenos toplote iz vročega na hladni medij, pri tem pa je prenos toplote izveden brez mešanja medijev. Tekom dobe trajanja toplotnega izmenjevalca le-ta prenaša ciklične tlačne obremenitve, ki so vzrok za porušitev lotnih spojev med dvema pločevinama toplotnega izmenjevalca iz materiala 316L (poznano tudi kot nerjavno jeklo 1.4404). V tem delu je opisana študija obnašanja lotnih spojev pod dinamično obremenitvijo. Na visokofrekvenčnem pulzatorju Vibrophore 100 so bili izvedeni utrujenostnih testi lotnih spojev pri različnih amplitudah in obremenitvenemu razmerju $R = 0{,}1$. Na podlagi dobljenih rezultatov je bil definiral materialni model lotnega spoja, ki je bil naknadno validiran z numeričnimi simulacijami znotraj programskega paketa Ansys. Razviti materialni model bo tako uporaben za bodoče trdnostne analize ploščnega toplotnega izmenjevalca.

Ključne besede: toplotni izmenjevalec, lotni spoj, utrujanje, eksperimentalno testiranje

## 1 INTRODUCTION

In different engineering applications we can find a lot of machines that are capable of transferring heat from hot to cold water. Because of many factors (the needs of industry, world population growth, etc.), the total number of those machines increases every year, which results in intensive technical progress. Machines that transfer heat are called heat exchangers and are used in many areas of everyday life. Heat exchangers can be used for the central heating of houses, the heating of domestic water, and many other purposes, including provision for different industries, e.g., the food industry, the pharmaceutical industry, and others.[1,2]

Due to high applicability, there are many different types of heat exchangers. Even though they all do the same tasks (transferring heat), they use different methods to execute the task. On a base level we can divide all the heat exchangers into two separate groups, which are recuperators and regenerators. In the first case, the heat is transferred from hot to cold water simultaneously, while in the second case, a time delay due to the heat-transfer method is used.[3] According to the aggregate state of the heat transferring medium, we also know single-phase and multi-phase heat exchangers. In this study, a single-phase heat recuperator will be analysed. In the case of this type of heat exchanger, both media have the same chemical composition (water), and they do not mix with each other.[3,4]

When it comes to different types of heat exchangers, we also know many geometrical designs, depending on the heat-transfer method and many other factors, including the type of medium, the intensity of the heat transfer, etc.[4] In this study, a plate heat exchanger (PHE) will be used. The PHE's geometrical design and mode of operation are shown in **Figure 1**.

This type of PHE consists of many parallel plates separating the hot and cold channels of the PHE. The number of plates and the plate thickness greatly depend on the power of different PHEs, which are needed for a certain scope of application.[4] In this study, the stainless steel 1.4404 (copper-brazed 316L) is used as a plate material. As connecting elements, which connect plates together inside the heat exchanger, brazed joints are being used.

*Corresponding author's e-mail:
srecko.glodez@um.si (Srečko Glodež)

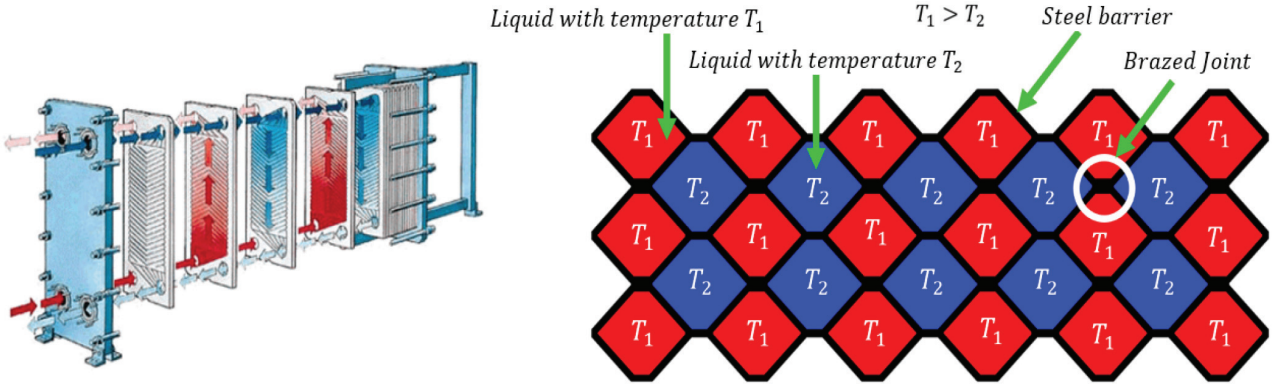


**Figure 1:** Geometry of PHE under consideration[5]

**Table 1:** Chemical composition of the steel 1.4404 in *w*/% according to the EN 10088-3

| C | Si | Mn | P | S | Cr | Mo | Ni | N |
|---|---|---|---|---|---|---|---|---|
| ≤ 0.03 | ≤ 1.0 | ≤ 2.0 | ≤ 0.045 | ≤ 0.015 | 16.5-18.5 | 2.0-2.5 | 10.0-13.0 | ≤ 0.11 |

A brazed joint is a type of connection that is formed when two points of material are pressed together while exposed to non-stationary temperature in a good vacuum. This process is also known as vacuum brazing and is commonly used in the PHE industry. Vacuum brazing is a jointing process that is accomplished at high temperatures, usually between 930 °C and 1230 °C, using a pure copper or nickel base alloy as the filler material.[6,7] In this production technology, a lower residual oxygen level inside the vacuum is achieved, and the contamination of parts is prevented. Here, the naturally formed oxide layers on the base metals can be decomposed in a vacuum at high temperatures, and it provide better joint properties such as high strength and less porosity through enhanced wetting. Additionally, vacuum brazing is favourable for lean and agile manufacturing due to the repeatability and reliability of brazed joints. In order to have a high-quality brazed joint, the parts must be closely fitted, and the base metal surfaces must be well cleaned. Here, the suitable clearance between braising parts should be a maximum of 0.1 mm in order to reach a good capillary effect. Brazing-surface cleanliness is very important since the contaminations on the surface can lead to insufficient wetting.[8]

Due to possible defects resulting from the manufacturing process, the brazed joint itself represents a possible weak spot where failure may occur. The failure occurs as a consequence of pressure inside the liquid medium and the presence of manufacturing defects. As a result of pressure changes in a liquid medium (water), a dynamic tensile force is applied to a brazed joint. When failure occurs in one of the PHE's brazed joints, the tensile stress on the remaining brazed joins in the surrounding area increases, which leads to a higher possibility of failure in those joints. With the increasing number of failures in brazed joints, the lifetime of the PHE decreases.[9]

In addition to the material's mechanical properties, the strength of brazed joints is also greatly influenced by the dynamic character of the tensile load, which also varies with different applications of use and types of PHEs. To define the dynamic character of the tensile force acting on a brazed joint, the appropriate loading ratio $R$ should be applied. Furthermore, the amplitude stress level must also be considered because it has a significant impact on the fatigue behaviour of the analysed brazed joint.[10] There are also many other factors that can have, in some cases, a great impact on the lifetime of a PHE: surface roughness, loading frequency, notch effects, temperature, etc.[11] In this study we focused on the constant loading frequency, constant temperature (all tests were performed at room temperature) and constant surface roughness. In that respect, a special specimen has been constructed to analyse the mechanical and fatigue properties of brazed joints for subsequent use in different applications of PHE. Furthermore, a material model of the analysed brazed joint has been developed, which enables further computational simulations of the PHEs made with brazing joint technology.

## 2 EXPERIMENTAL TESTING

### *2.1 Specimen preparation*

The test specimen shown in **Figure 2** was prepared using the same manufacturing process (vacuum brazing) as normally used when making brazed joints in PHEs (see also Section 1). Here, two bars made of stainless steel 1.4404 (see **Table 1**) were vacuum brazed using a copper foil with a thickness of 0.1 mm.

### *2.2 Quasi-static tests*

Quasi-static tests were made on a Zwich/Roel Vibrophore 100 testing machine. Four quasi-static tensile tests were made to obtain the engineering $\sigma$–$\varepsilon$ diagram of

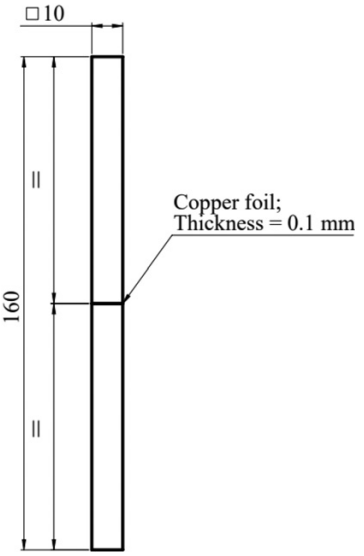


**Figure 2:** Geometry of test specimens

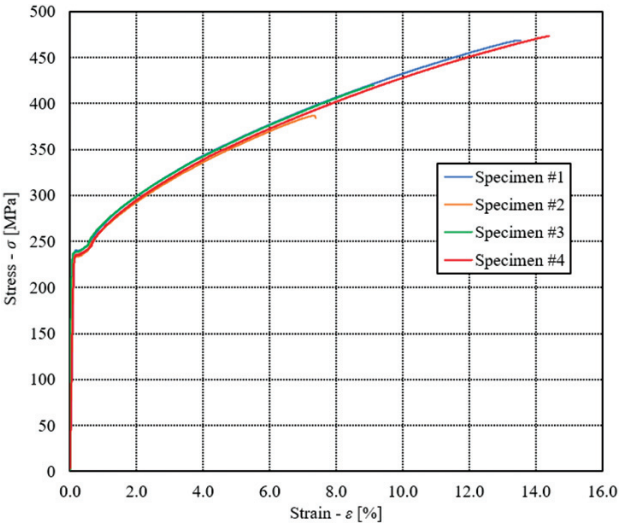


**Figure 3.** Engineering diagram $\sigma$–$\varepsilon$ of quasi-static tests[5]

the analysed brazed joint. The quasi-static tests were displacement-controlled using a mechanical extensometer with a constant displacement rate of 0.5 mm/min up to the final fracture of the specimen. The results for all four tests are presented in **Figure 3** and summarised in **Table 2**.

The axial deformation of the test specimen is a combination of the axial deformation of the steel pieces and the copper part in the middle of the test specimen. However, the volume of the copper part in the middle of the test specimen is practically negligible if compared to the volume of the steel pieces. It is, therefore, reasonable that the majority of the total axial deformation is due to the elongation of the steel part of the test specimen. For the same reason it is also reasonable to expect the value of the modulus of elasticity to be approximately equal to that of the base material of the test specimen (200 GPa for the selected stainless steel). The same is also valid for the yield stress and tensile strength of the analysed brazed joint.

Based on the average values of the mechanical properties presented in **Table 2**, the average engineering stress–strain curve ($\sigma_{eng}$–$\varepsilon_{eng}$) was obtained. However, the true stress–strain curve ($\sigma_{true}$–$\varepsilon_{true}$) should be applied when creating the material model of the analysed brazed joint (see Section 4). Therefore, the following equations should be used to make this transformation:[12]

$$\varepsilon_{true} = \ln(1+\varepsilon_{eng}) \quad (1)$$

$$\sigma_{true} = \sigma_{eng}(1+\varepsilon_{eng}) \quad (2)$$

When creating the material model of the analysed brazed joint, the elastic part of the true stress–strain curve can be given by the Youngs' modulus $E$ (see **Table 2**). Therefore, only the plastic part should be defined as a data pair ($\sigma_{true}$–$\varepsilon_{true}$).

### *2.3 Fatigue tests*

Fatigue tests were made on the same machine as the quasi-static tests (Zwich/Roel Vibrophore-100) using the same specimens (see **Figure 2**). The fatigue tests were performed at a temperature of 20 °C under a loading ratio $R$ = 0.1 and a loading frequency of approximately 98 Hz. All the tests were performed in the high-cycle fatigue regime (HCF), which means that the maximum stress in each loading cycle did not exceed the yield stress of the analysed braised joint (i.e., $R_e$ = 237 MPa, see **Table 2**). Following this limitation, the maximum tensile stress of (0.6–0.8)·$R_e$ was selected. **Figure 4** shows the S–N plot of fatigue tests where the amplitude stress $\sigma_a$ is given on the ordinate axis.

As already explained above, the fatigue tests were performed under a loading ratio $R$ = 0.1. It means that

**Table 2:** Mechanical properties of the analysed brazed joint

| | Youngs modulus | Poissons ratio | Yield stress | Ultimate tensile stress | Elongation |
|---|---|---|---|---|---|
| Specimen No. | $E$ (MPa) | $\nu$ (–) | $R_e$ (MPa) | $R_m$ (MPa) | $EL$ (%) |
| #1 | 200,049 | 0.28 | 240 | 469 | 13.5 |
| #2 | 197,472 | 0.28 | 234,5 | 387 | 7.4 |
| #3 | 196,078 | 0.28 | 238 | 420 | 9.1 |
| #4 | 199,951 | 0.28 | 235,5 | 473 | 14.4 |
| Average | **198,387** | **0.28** | **237** | **437** | **11.1** |

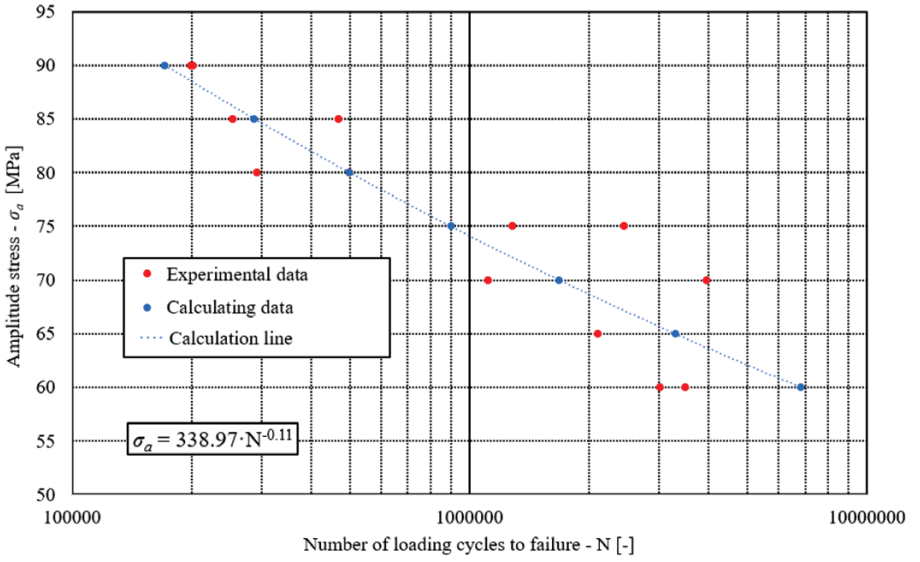


**Figure 4:** S–N plot of the analysed brazed joints[5]

for each amplitude stress $\sigma_a$, the belonging mean stress $\sigma_m$ can be obtained as follows:

$$\sigma_m = \frac{\sigma_a (1+R)}{1-R} \tag{3}$$

However, the standardised fatigue tests of different engineering materials are usually performed with zero mean stress (i.e., $\sigma_m = 0$; $R = -1$). With that respect, the fatigue material parameters of engineering materials taken from the literature are usually related to the zero mean stress. For that reason, the S-N curve for $R = 0.1$ presented in **Figure 4** could be transformed into the S–N curve for $R = -1$ using the Goodman equation:[13,14]

$$\sigma_a (R = 0.1) = \sigma_D \left[1 - \frac{\sigma_m}{R_m}\right] \tag{4}$$

where $\sigma_D$ is the fatigue strength for $R = -1$ and $R_m$ is the ultimate tensile stress of the analysed braised joint. Considering the average ultimate tensile strength of the analysed brazed joint $R_m \approx 437$ MPa (see **Table 2**), the following data pairs for zero mean stress can be defined:

$N_1 = 171269$ $\quad \sigma_{a1} = 90$ MPa $\quad \sigma_{D1} = 120.3$ MPa

$N_2 = 6822251$ $\quad \sigma_{a2} = 60$ MPa $\quad \sigma_{D2} = 72.1$ MPa

When analysing the fatigue problems of engineering components and structures, the Basquine equation is normally used to describe the S–N curve:

$$\sigma_{true} = \sigma_{eng} (1 + \varepsilon_{eng}) \tag{5}$$

where $\sigma_f$' is the fatigue-strength coefficient and $b$ is the fatigue-stress exponent. Considering the data pairs ($N_1$, $\sigma_{D1}$) and ($N_2$, $\sigma_{D2}$) as described above, the material parameters $\sigma_f$' and $b$ for zero mean stress (i.e., $\sigma_m = 0$; $R = -1$) result in $\sigma_f$' = 706.1 MPa and $b = -0.139$. These parameters will then be considered when creating the fatigue material model of the analysed brazed joint (see Section 3).

## 3 NUMERICAL MODELLING

The numerical modelling of the analysed brazed joints was performed using Ansys software, where the simplified geometry of the brazed joint specimen was applied for that purpose. In this case, the numerical model was built as a solid homogeneous piece of the material with the same cross-section area as already used in the experimental testing (see **Figure 2**). However, only the measuring length of the specimen (i.e., 50 mm) was considered for the subsequent numerical computations.

In the material section of the Ansys database, the new material was defined. It had the same mechanical properties as obtained in the framework of the experimental testing. Here, it should be pointed out that all the mechanical properties were applied at room temperature $\vartheta_0 = 20$ °C. In the next step, all the boundary conditions of the numerical model were obtained in order to perform the proper numerical simulation. In that respect, certain degrees of freedom in the numerical model were limited by setting some displacement values to zero. Furthermore, external loading was applied indirectly by the non-zero values of the displacement on the front surface of the numerical model (see **Figure 5**). These values of the displacement should be large enough to reach an engineering stress that is higher than the yield strength of the material (i.e., analysed braised joint), resulting in plastic strain. The described loading procedure was only used to perform static numerical simulations to confirm the experimental results obtained previously with tensile tests (see Section 2.2).

In the case of the numerical simulation of the fatigue loading, different values of the tensile force were prescribed on the same surface, as explained above for the quasi-static numerical simulation. Here, the maximum tensile force and, consequently, different levels of amplitude stress were defined for each simulation considering

| | Steps | Time [s] | Z [mm] |
|---|---|---|---|
| 1 | 1 | 0, | 0, |
| 2 | 1 | 1, | 0,5 |
| 3 | 2 | 2, | 1, |
| 4 | 3 | 3, | 1,5 |
| 5 | 4 | 4, | 2, |
| 6 | 5 | 5, | 2,5 |
| 7 | 6 | 6, | 3, |
| 8 | 7 | 7, | 3,5 |
| 9 | 8 | 8, | 4, |
| 10 | 9 | 9, | 4,5 |
| 11 | 10 | 10, | 5, |
| 12 | 11 | 11, | 5,5 |
| 13 | 12 | 12, | 6, |
| 14 | 13 | 13, | 6,5 |
| 15 | 14 | 14, | 7, |

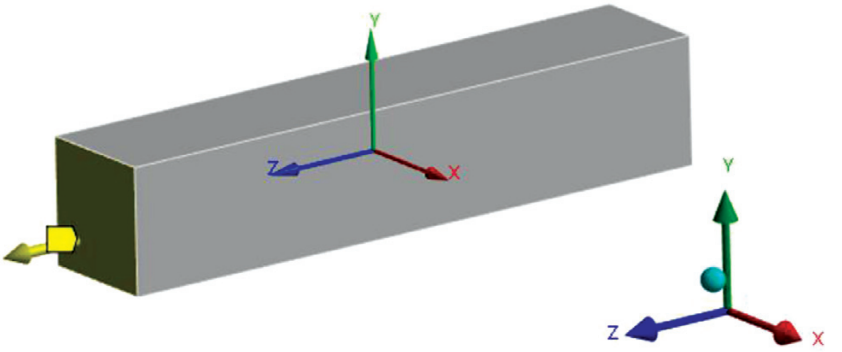


**Figure 5:** Applied load case for the static numerical simulation

the loading ratio $R = 0.1$ and Goodmann's model to evaluate the mean stress effect. In computational modelling, a standard Ansys finite element type SOLID 186 was selected. This is a 3D quadratic finite element that has a cuboid shape.[15,16] After the comprehensive mesh-convergence analysis, a FE mesh with a FE size of 1 mm was used.

The numerical model, as described above, was then used for the subsequent numerical simulations. In the first step, the quasi-static numerical simulation was performed to obtain the engineering $\sigma$–$\varepsilon$ diagram (see **Figure 6**). Here, the reaction forces acting in the opposite direction with regard to the external loading were obtained in each loading step and then divided by the cross-section area of the specimen.

When creating the fatigue material model of the analysed brazed joint, the characteristic data pairs ($\sigma_a$, $N$) taken from the trendline of the S–N plot in **Figure 4** (see **Table 3**) were considered. For this purpose, we converted the values of amplitude stress $\sigma_a$ from **Table 3** to values of maximum stress $\sigma_{max}$ and then calculated the number of cycles $N$ for the load ratio $R = 0.1$ using Goodman's equation to consider the mean stress effect. **Figure 7** shows the S–N plot of the fatigue numerical simulation as described above.

**Table 3:** Calculated data pairs ($\sigma_a$, N) taken from the trendline of the S–N plot in **Figure 4**

| Amplitude stress $\sigma_a$ (MPa) | Number of loading cycles $N$ (–) |
|---|---|
| 90 | 171269 |
| 85 | 287917 |
| 80 | 499498 |
| 75 | 897941 |
| 70 | 1680899 |
| 65 | 3296275 |
| 60 | 6822251 |

## 4 RESULTS AND DISCUSSION

**Figure 8** shows the comparison between the experimental and computational results for the engineering diagram $\sigma$–$\varepsilon$. It is evident that for all the considered experimental tests the yield stress was around 237 MPa, which corresponds to the numerical simulations. In the elastic area (below the yield stress) a very good match between the experimental and numerical results was observed.

However, in the plastic area (above the yield stress), more mismatches appeared, especially in the case of the ultimate tensile strength. It is clear that the ultimate strength determined by the numerical simulation was around 437 MPa, which corresponds to the average value

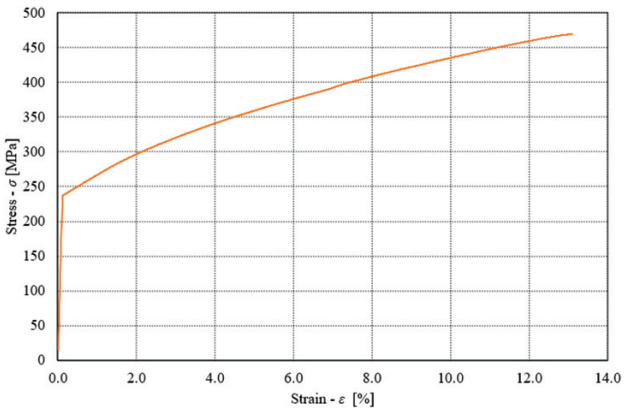


**Figure 6:** Numerical determination of the engineering diagram $\sigma$–$\varepsilon$

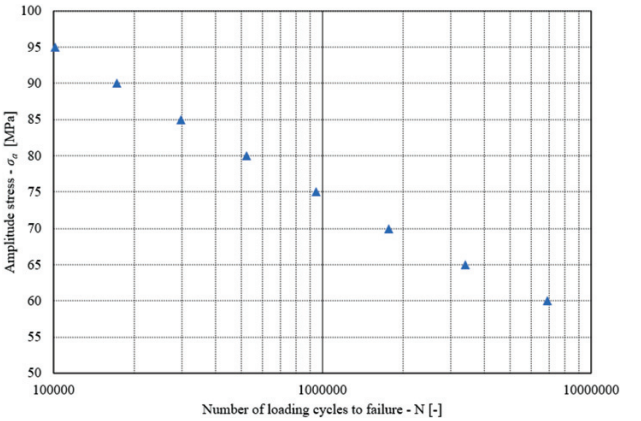


**Figure 7:** S–N plot of the fatigue numerical simulation

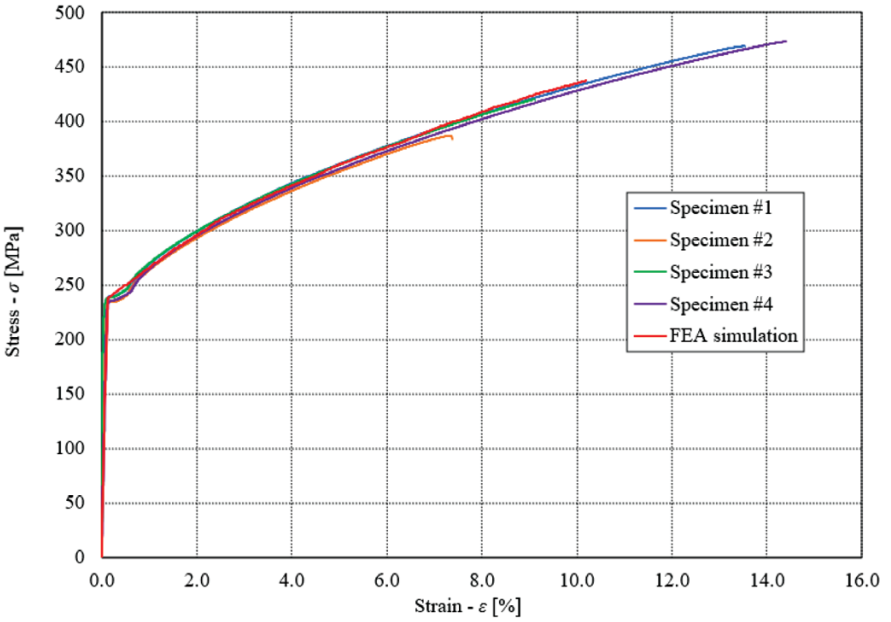


**Figure 8:** Experimentally and computationally obtained engineering diagram $\sigma$–$\varepsilon$

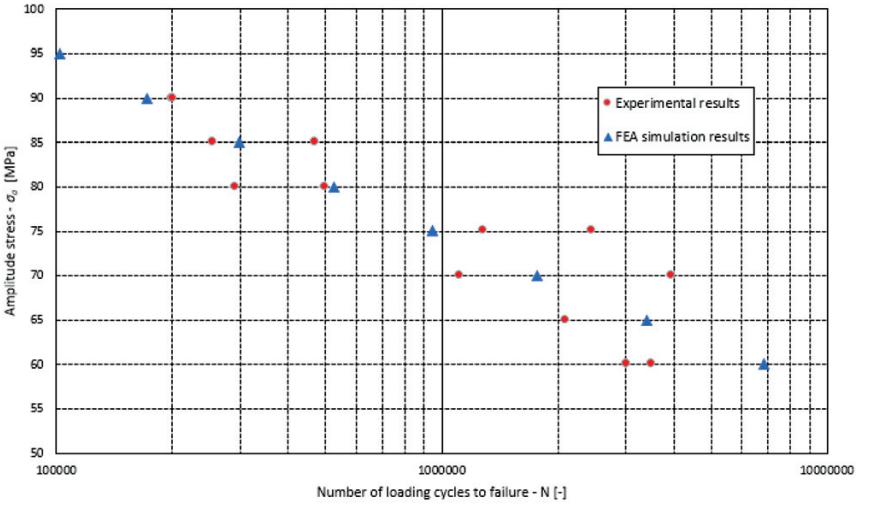


**Figure 9:** Experimentally and computationally obtained S–N plot for $R$ = 0.1

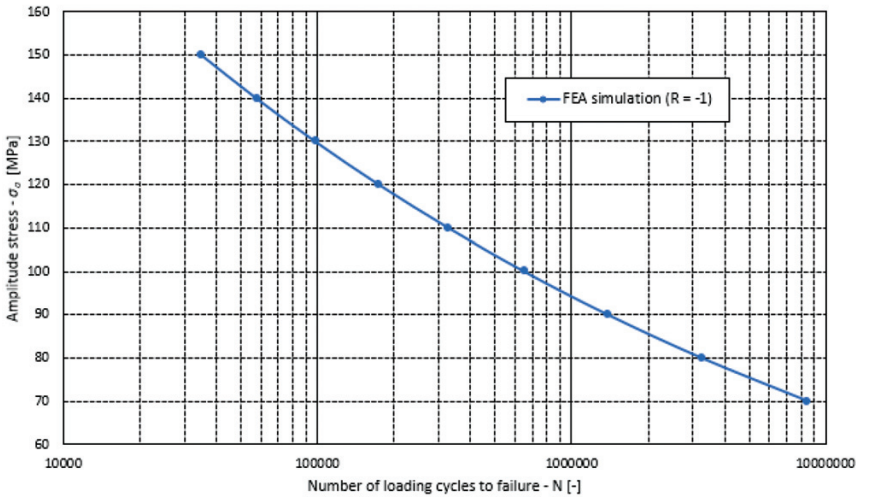


**Figure 10:** Computationally obtained S–N plot for $R$ = –1 (i.e., $\sigma_m$ = 0)

of the ultimate tensile strength obtained experimentally. Considering this fact, the material model for the quasi-static loading of the analysed braised joint was validated.

**Figure 9** shows a comparison between the experimental and computational results for the fatigue loading(S–N plot) of the analysed brazed joint. In both cases, the fatigue life (i.e., the number of cycles $N$ until failure) increased with a decrease in the amplitude stress $\sigma_a$. However, the scatter of the experimental results is much wider if compared to the quasi-static loading. This is probably due to a greater impact of the manufacturing errors on the fatigue strength occurring during the manufacturing process of the specimens. On the other hand, the computational results are still a good representation of the experimental results, which validate the material model for the fatigue evaluation.

In the case of the loading ratio $R = 0.1$, the mean stress level is not constant for all levels of the amplitude stress. The constant value of the mean stress can be achieved by adjusting the loading ratio $R$ to the value –1 (i.e., zero mean stress). As the amplitude stress $\sigma_a$ changes, the mean stress remains zero; therefore, it is possible to determine the number of loading cycles at different values of $\sigma_a$ and zero mean stress. The S–N curve of the analysed brazed joint for zero mean stress is presented in **Figure 10**.

## 5 CONCLUSION

For the purpose of this study, tensile experimental testing of brazed joint specimens was conducted. In the first phase, quasi-static testing was performed to define the engineering $\sigma$–$\varepsilon$ curve. Furthermore, comprehensive fatigue tests under a pulsating loading (load ratio $R = 0.1$) were performed to obtain the S–N curve of the analysed brazed joints. Based on the theoretical study, experimental testing, and comprehensive numerical analyses, the following conclusions can be drawn:

In the case of quasi-static testing, the yield stress varied between 235 MPa and 240 MPa for all the tested specimens. Therefore, the average value $R_e = 237$ MPa was obtained as the yield stress of the analysed brazed joint. On the other hand, different values of the ultimate tensile stress $R_m$ ranging between 387 MPa and 473 MPa were obtained for the individual specimens.

Based on the obtained experimental results, an average engineering $\sigma$–$\varepsilon$ curve was created and then divided into individual linear segments. For the purpose of the subsequent computational analyses, the amount of elastic strain was subtracted from the total strain in the true $\sigma$–$\varepsilon$ diagram.

In the second phase, the fatigue testing under load ratio $R = 0.1$ at a temperature of 20 °C was performed to obtain the S–N plot of the analysed brazed joint. Furthermore, the Goodman mean stress correction was applied to express the obtained experimental results for the load ratio $R = –1$ (i.e., for the zero mean stress), which usually appears when presenting the fatigue properties of engineering materials in the literature.

The material model was validated with a numerical analysis using the Ansys software. A validated material model can then be used for the subsequent numerical analysis of PHE in different engineering applications.

## Acknowledgements

The authors acknowledge the financial support of the Research Core Funding (No. P2-0063) and the Basic Postdoc Research Project (No. Z2-50082) from the Slovenian Research Agency. The authors also acknowledge for the use of research equipment High-Frequency Pulsator, procured within the project "Upgrading national research infrastructures – RIUM", which was co-financed by the Republic of Slovenia, the Ministry of Education, Science and Sport and the European Union from the European Regional Development.

## 6 REFERENCES

[1] H. A. Zahid, Plate heat exchanger literature survey and new heat transfer and pressure drop correlations for refrigerant evaporators, Heat transferring engineering, 24 (**2010**), 3–16

[2] Y. Gürler, Design and mechanical behaviour of brazed plate heat exchangers, MSc thesis, Izmir Institute of Technology, 2018

[3] G. F. Hewitt, G. L. Shires, T. R. Bott, Process Heat Transfer, CRC Press, New York, 1994

[4] Y. Mizokami, T. Igari, F. Kawashima, N. Sakakibara, M. Tanihira, T. Yuhara, T. Hiroe, Development of structural design procedure of plate-fin exchangers for HTGR, Nuclear engineering and design, 255 (**2013**), 248–262

[5] B. Hanželič, J. Kralj, T. Bončina, B. Nečemer, J. Kramberger, R. Satošek, S. Glodež, Fatigue Behaviour of Brazed Joints for Heat Exchangers. Materials, 17 (**2024**) 2, 479

[6] M. P. Groover, Fundamentals of Modern Manufacturing, New Jersey: JohnWiley & Sons, 2010

[7] J. Kowalewski, J. Szczurek, Issues in vacuum brazing, ASM International, Dallas, 2006

[8] M. M. Schwartz, Brazing, ASM International, Ohio, 2003

[9] K. Takeshita, Y. Terakura, A novel approach for predicting the tensile strength of brazed joints, Metallurgical and materials transactions A, 29 (**1998**), 587–592

[10] V. Fedorov, T. Uhlig, G. Wagner, Investigation of fatigue damage in aluminium/stainless steel brazed joints, Welding in the world, 62 (**2018**), 609–616

[11] Y. Hayta, Investigation of the fatigue behaviour of metallic components used in plate heat exchangers under variable dynamic loads. Graduate School of Engineering and Science of Izmir Institute of Technology, 2020

[12] A. Petrik, R. Aroch, Usage of true stress – strain curve for FE simulation and the influencing parameters. IOP Conference Series Materials Science and Engineering, 566 (**2019**) 1, 2025

[13] O. Gyojo, Effective stress and fatigue life prediction with mean stress correction models on a ferritic stainless-steel sheet, International Journal of Fatigue, 157, (**2022**), 106707

[14] S. Kwofie, An exponential stress function for predicting fatigue and life due to mean stresses. International Journal of Fatigue, 23, (**2001**), 829–836

[15] ME 304 Finite Element Analysis Basic types of FEA Elements. Available at: https://faculty.up.edu/lulay/ME304/ANSYS-BasicElements-line-2D-3D.pdf (25.9.2023)
[16] C. Xiaolin, L. Yijun, Finite Element Modeling and Simulation with ANSYS Workbench. CNC Press, 2019